LDEF YAW AND PITCH ANGLE ESTIMATES

Bruce A. Banks
NASA Lewis Research Center
Cleveland, Ohio

Linda Gebauer
Cleveland State University
Cleveland, Ohio

INTRODUCTION

Quantification of the LDEF yaw and pitch misorientations is crucial to the knowledge of atomic oxygen exposure of samples placed on LDEF. Video camera documentation of the LDEF spacecraft prior to grapple attachment, atomic oxygen shadows on experiment trays and longerons, and a pinhole atomic oxygen camera placed on LDEF provided sources of documentation of the yaw and pitch misorientation. Based on uncertainty-weighted averaging of data, the LDEF yaw offset was found to be 8.1 ± 0.6°, allowing higher atomic oxygen exposure of row 12 than initially anticipated. The LDEF pitch angle offset was found to be 0.8 ± 0.4°, such that the space end was tipped forward toward the direction of travel. The resulting consequences of the yaw and pitch misorientation of LDEF on the atomic oxygen fluence is a factor of 2.16 increase for samples located on row 12, and a factor of 1.18 increase for samples located on the space end compared to that which would be expected for perfect orientation.

ACKNOWLEDGMENT

The authors gratefully acknowledge the assistance of Robert O'Neal of the Langley LDEF Project Office who greatly contributed to the assessment of the LDEF yaw and pitch orientation.

YAW OFFSET

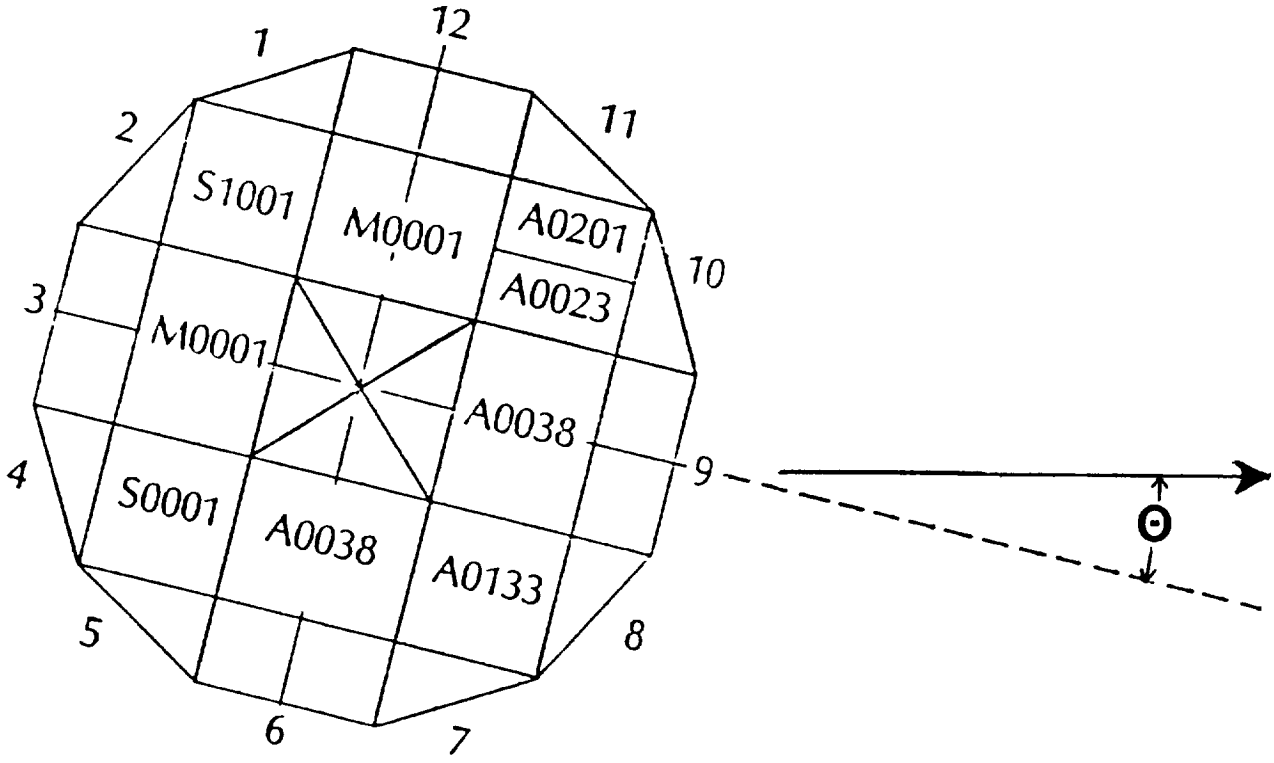

Viewgraph #2:

For the purposes of this investigation, a positive yaw offset is a rotation of the LDEF spacecraft about its long axis in a clockwise direction as viewed from above looking down at the space end.

LDEF YAW MISORIENTATION

	Source	LDEF Yaw Misorientation, degrees (Allowing Greater Atomic Oxygen Exposure of Row 12 Than Row 6)	Uncertainty, Degrees
Video Camera Documentation of Cloud Movement relative to LDEF prior to grapple attachment	Banks, NASA LeRC	8.3	± 1.1
Shadows behind on Earth End	Banks, NASA LeRC	7.0	± 1.4
Pin Hole Camera	Gregory, University of Alabama in Huntsville	8.0	± 0.4
Nut Plate Shadows on Longerons	Banks, NASA LeRC	4.3	± 1.0
Nut Plate Shadows on Tray 9C	Banks, NASA LeRC	7.4	± 0.5
Nut Plate Shadows on Transverse Flat-Plate Heat Pipe Experiment S1005	Linton & Vaughn, NASA MSFC	11.0	± 1.0
Nut Plate Shadows on Solar Array Materials Passive LDEF Experiment A0171	Linton & Vaughn, NASA MSFC	12.0	± 1.0
Nut Plate Shadows on Thermal Control Surfaces Experiment S0069	Linton & Vaughn, NASA MSFC	11.5	± 1.0

Viewgraph #3:

This table lists the various yaw offsets measured by LDEF investigators. The first measurement listed and the fourth through the eighth measurements will be discussed later. The second measurement listed is that of the atomic oxygen shadows of both heads on the LDEF's earth end. The third measurement listed is that of Dr. John Gregory's pinhole camera. This was the only device on the LDEF spacecraft which was specifically intended to measure the LDEF's orientation. The pinhole camera consisted of a 0.5 mm (0.020") diameter pinhole in a 3.25 cm (1.28") radius silver-coated stainless steel hemisphere. Although the silver was highly oxidized as a result of overexposure caused by scattered atomic oxygen, a clear visualization of the arrival direction of atomic oxygen was observed. The uncertainties listed are probable errors.

Viewgraph #4:

This picture is a copy of the video camera photos prior to retrieval. The orientation of the LDEF spacecraft was noted by observing the tray edges on the space end. The direction of travel of the LDEF spacecraft with respect to ground is noted by the specific cloud formations.

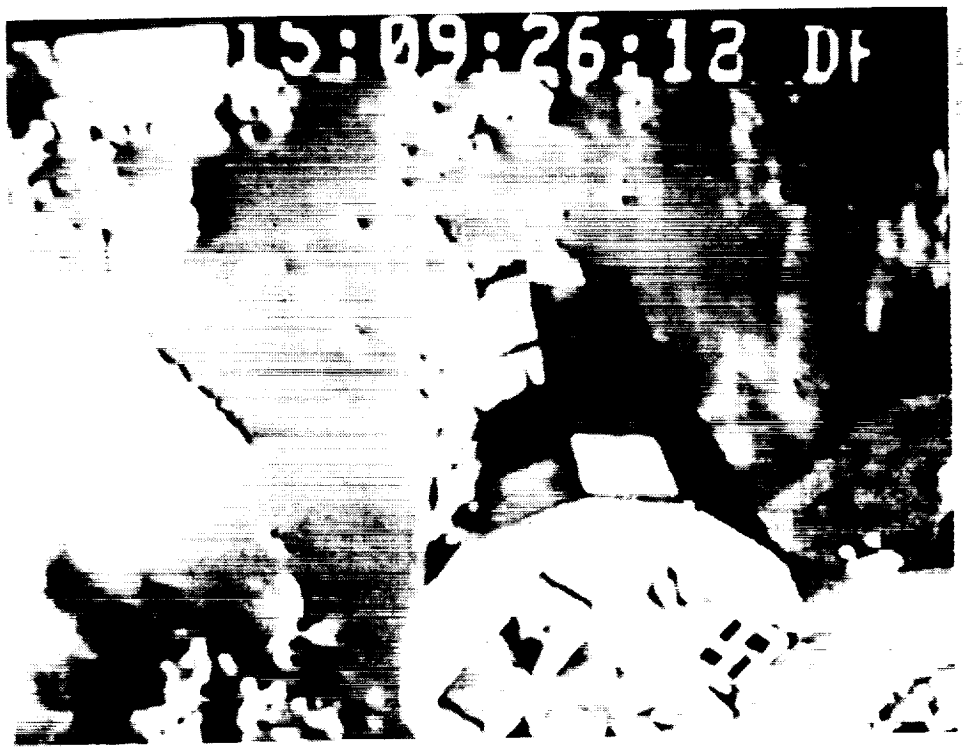

Viewgraph #5:

This photo shows the LDEF spacecraft 22 seconds after the prior photo. Note some of the same cloud formations can be seen displaced from their previous positions. Lines that were drawn connecting the cloud formation allowed the direction of travel to be measured with respect to the LDEF orientation. To properly perform this measurement, corrections were made to account for the angle under which the LDEF spacecraft was observed to predict what the actual yaw offset would be. As can be seen from the previous yaw offset summary table, the video camera yaw misorientation was in agreement with the pinhole camera and shadows behind both heads on the earth end if one considers the uncertainties.

Viewgraph #6:

This photo shows the openings in the tray corners, as well as the nut plates on the tray flanges, which were used pre- and post-flight to attach protective covers over the experiments.

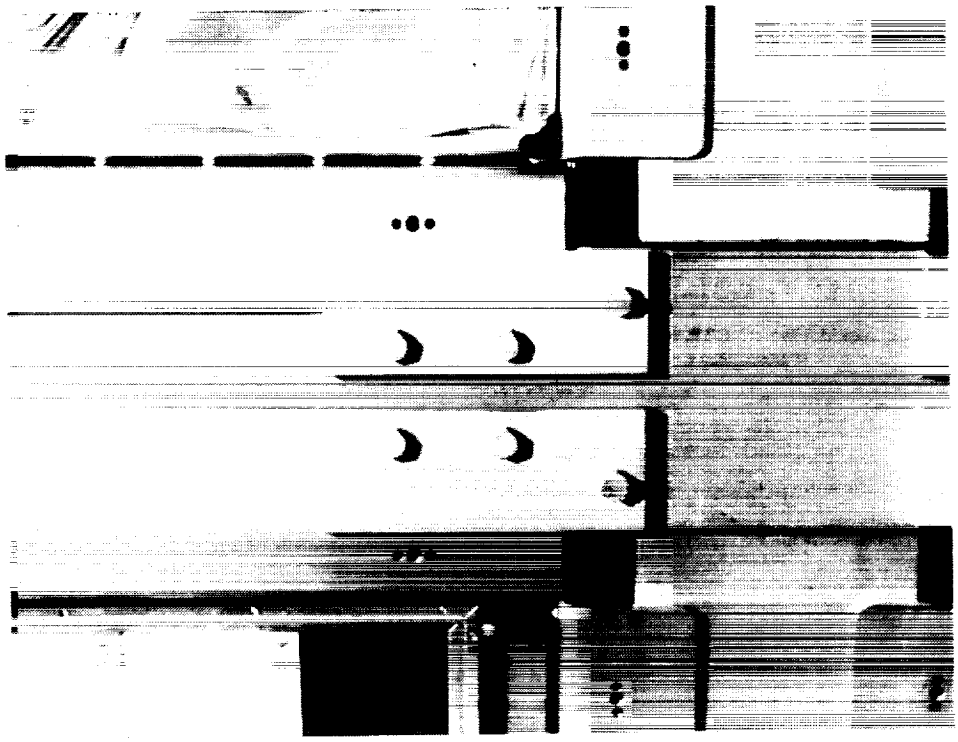

Viewgraph #7:

This photo shows the detailed configuration of typical tray corner openings, and nut plates which had 10-32 screw hole apertures, allowing atomic oxygen to enter into the LDEF interior.

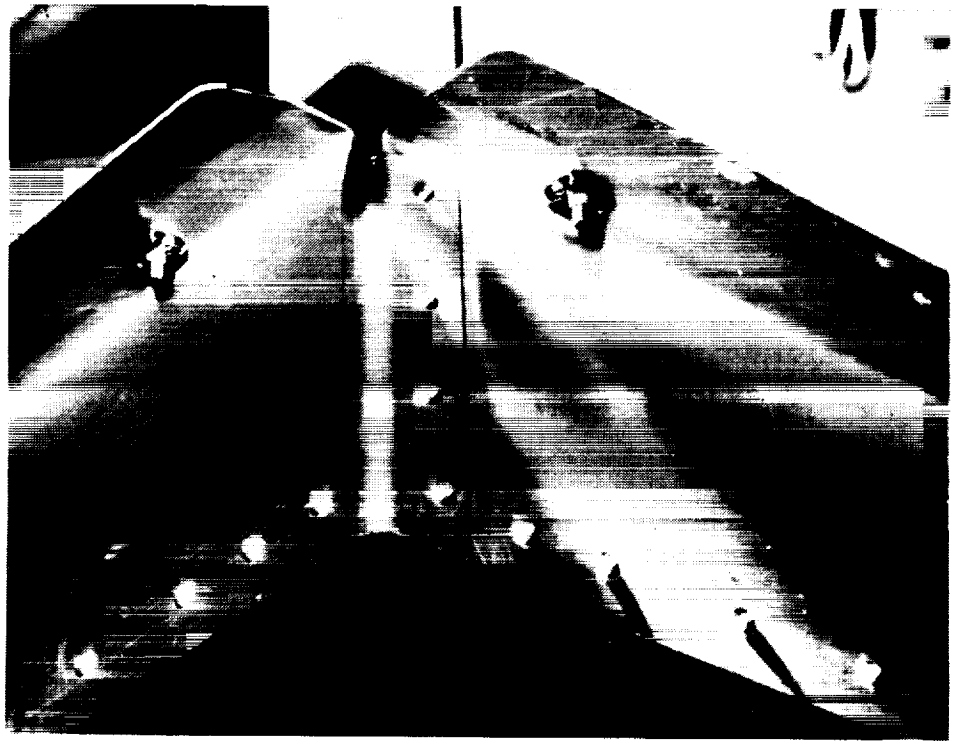

Viewgraph #8:

This photograph of an LDEF tray on row 11 bay A shows the typical atomic oxygen darkened contaminant streak on the LDEF tray sides as a result of atomic oxygen entrance into the LDEF interior through the openings in the corners of the trays. Note in this photo, the nut plates have the screws attached because the protective coverlet has been installed post-flight. The contaminant on this corner was analyzed and found to contain silicon, as well as carbon. Based on numerous other measurements, it is probable that silicone contaminants from within LDEF were oxidized to form silicates, which also contain other hydrocarbon contaminants. Note also that the rivet heads on the bottom of the tray make atomic oxygen shadows which point back to the direction of the opening of the tray.

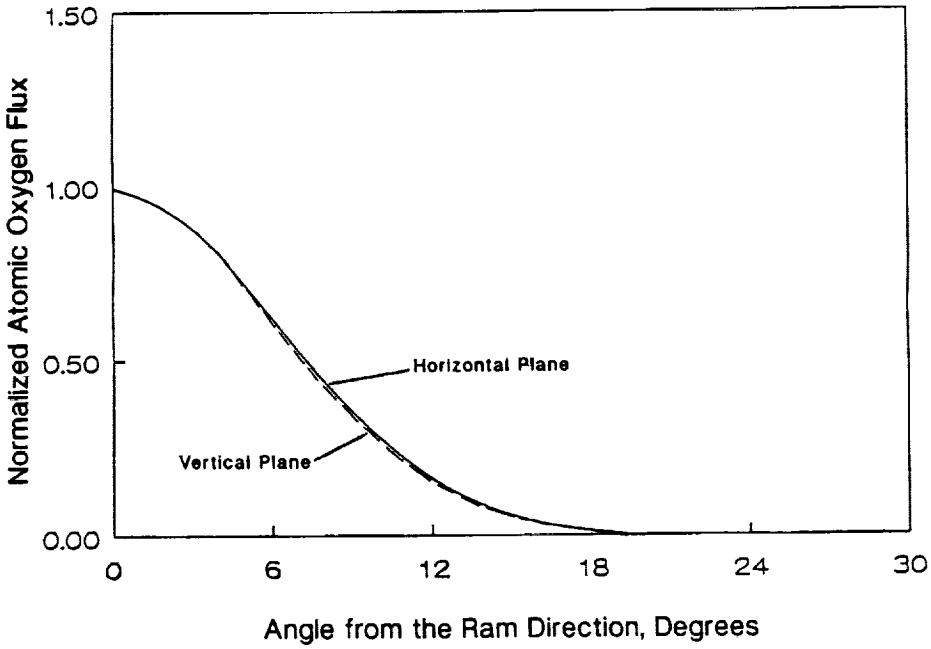

Viewgraph #9:

This plot shows the atomic oxygen arrival angular distribution for LDEF assuming 1227 K atoms, 411 kilometers altitude, and 28.5° orbital inclination. Because the atomic oxygen atoms are hyperthermal, arriving atomic oxygen has a distribution of arrival directions, causing the atomic oxygen streaks within the trays to be broad, rather than thin lines.

ATOMIC OXYGEN INCIDENT ANGULAR DISTRIBUTION

411 km altitude
1227 K atoms
28.5° inclination

Viewgraph #10:

This plot shows the same angular distribution plotted in polar coordinates.

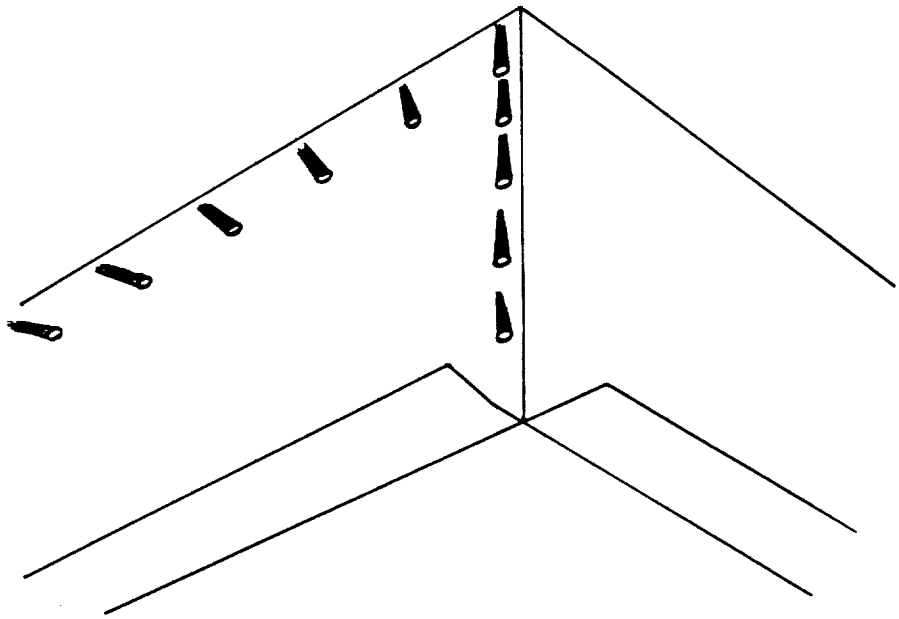

Viewgraph #11:

Because atomic oxygen arrives from a variety of incoming angles, all streaks behind the rivet heads on the tray point back to the opening, rather than specifically to the direction of the main arrival of atomic oxygen. The intensityof the streaks is perhaps a better measure of the direction arrival. That is to say, where the streaks are darkest are where the central arrival direction is most likely. Thus the broad distributed arrival of atomic oxygen through the tray corners does not allow accurate measure of the LDEF yaw orientation. The smaller openings of the 10-32 nut plates, on the other hand, did allow more accurate ground measurements.

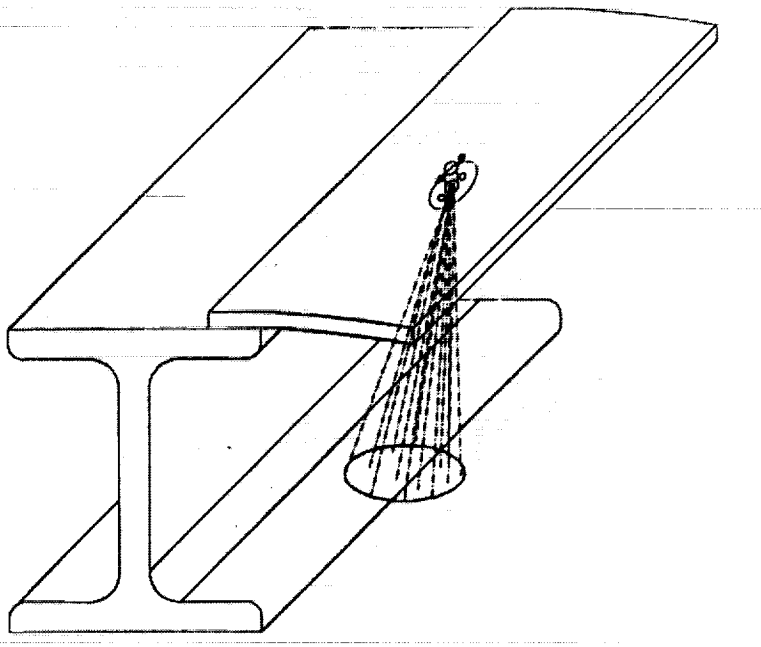

Viewgraph #12:

Nut plate measurement shadows on the longerons indicated a 4.3° yaw misorientation with a probable error of ±1°.

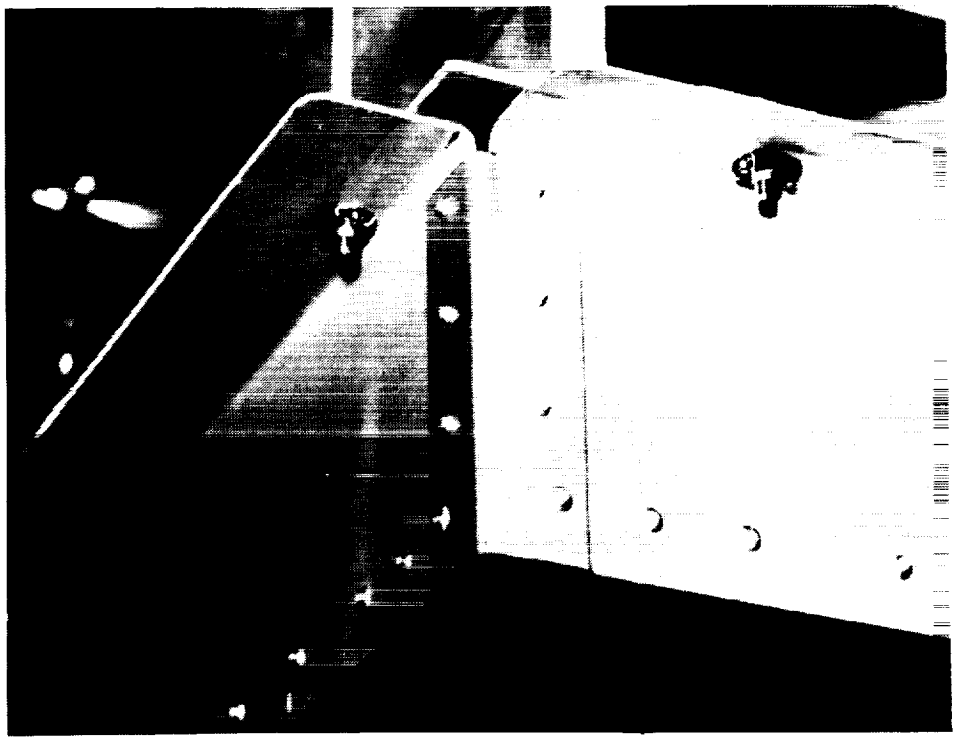

Viewgraph #13:

This photo of the LDEF tray from row 9, Bay C shows faint nut plate streaks which were useful for both the yaw and pitch measurements. Similar measurements from other trays were made by Roger Linton and Jason Vaughn of NASA Marshall Space Flight Center as well as the authors. The quality of the measurements relies heavily upon uniformity of arrival of silicone-containing contaminants. Areas of high spacial gradients in contaminant flux may have misoriented atomic oxygen streaks. Efforts were made by the author to measure only streaks which had high degrees of symmetry.

Generic Measurement	Yaw Misorientation (allowing greater atomic oxygen exposure of row 12)
Video Camera Documentation Prior to Grapple Attachment	8.3 ± 1.1
Shadows Behind Nuts on Earth End	7.0 ± 1.4
Pin Hole Camera	8.0 ± 0.4
Nut Plate Shadows	9.2 ± 1.0
AVERAGE	8.1 ± 0.6

Viewgraph #14:

This summary chart lists the generic types of yaw misorientation measurements. For each generic yaw misorientation measurement, the angles specified are the averages of all investigators' information with their assigned probable error estimates. The overall average is an uncertainty weighted average of the various generic measurements, along with its probable error.

PITCH OFFSET

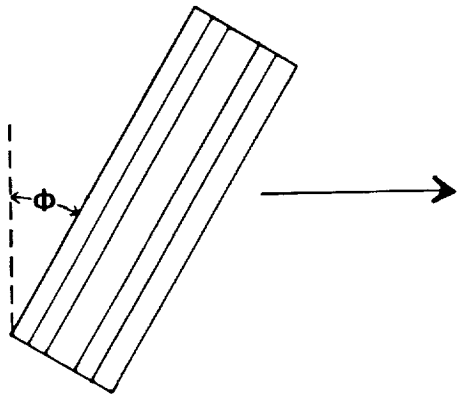

Viewgraph #15:

This drawing shows the LDEF as viewed from the side where the pitch angle is considered positive if the space end is leaning forward in the direction of travel.

LDEF PITCH ANGLE MISALIGNMENT DATA SOURCES

	Source	Pitch Angle, degrees (Space End Forward is +)
1.	Pinhole Camera from AO114 on 9C	1 ± 0.4
2.	Nut Plate Shadow on Longeron Flange under 9B	0 ± 1.0
3.	Scuff Plate Shadows from Trunnions on Row 9	No Shadows Observed
4.	Grapple Alignment Pin Shadow from 10C	No Shadows Observed
5.	Be^7 Populations on Space and Earth End Tray Clamps compared to those around LDEF	Not Measured
6.	Nut Plate Shadows on Tray Sides Parallel to Longerons on Tray 9C	0.66 ± .35
7.	Solar Absorptance of A-276 Paint Spots on Space and Earth Ends compared to around LDEF	-1.72 + 8.5 / -7.2 } Space End
		-40.5 + 4.6 / -3.9 } Earth End
8.	Shadows of Tray Corner Openings on LDEF Internal Structures	Data Unavailable
9.	Mass Model Gravity Gradient Stabilization Prediction of Pitch Angle	Data Unavailable
10.	Experiment Exposure Control Canister Drive Screw Shadows on S0010 on 9B	No Shadows Observed

Viewgraph #16:

This table shows the various sources of information for determination of the LDEF pitch angle. As can be seen, many of the potential sources of data revealed no results or data which had high probable errors relative to the magnitude of the measurement. The first source of information, the pinhole camera from Dr. John Gregory's experiment on AO114 on Row 9C, is one of the more definitive measurements. The pinhole camera was specifically designed to measure the LDEF spacecraft orientation, and had a measurement in excess of its probable error. On the other hand, the nut plate shadow on longeron flange under 9B had a probable error in excess of the measurement, and it therefore is deemed non-usable as a source of data. Atomic oxygen shadows from the trunnions on Row 9, and the grapple alignment pins on tray 10C were not observable, and therefore no information was gained from items 3 and 4. Similarly, because the Be^7 calculations were not measured on the space or earth end tray clamps, calculations of the pitch were not possible to be made to compare with the Be^7 calculations around LDEF. The nut plate shadows on the tray sides parallel to longerons on tray 9C did provide meaningful data. The solar absorptance from paint spots on the space and earth end produced highly uncertain data with questionable reliability based on contamination issues. Items 8, 9, and 10 had potential to provide information, however, no observations or data was found available to produce meaningful numbers.

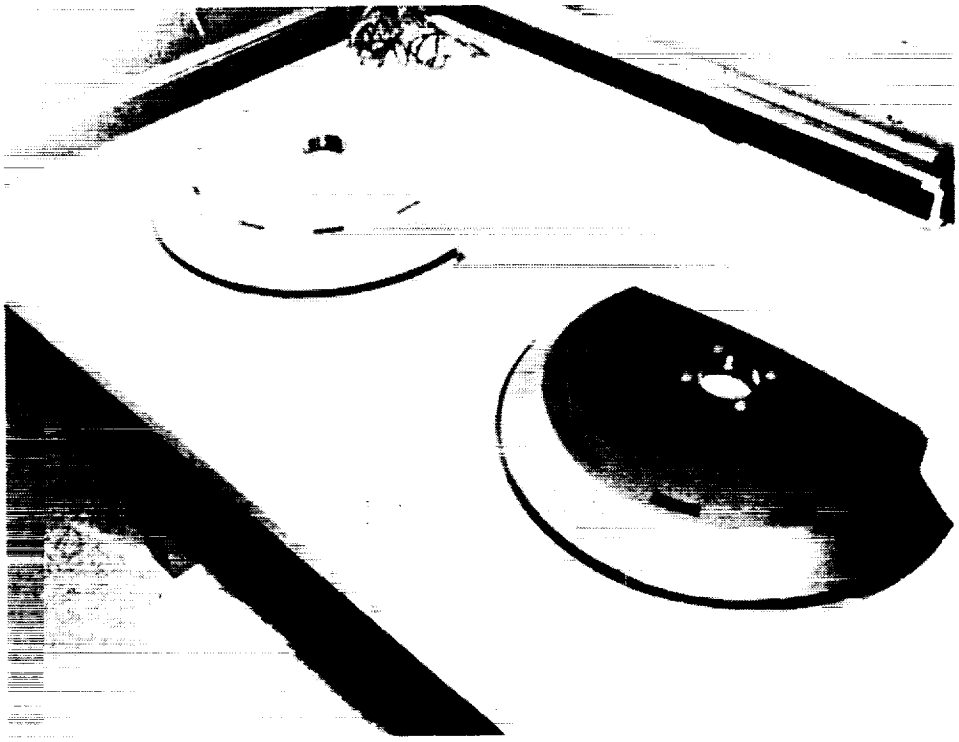

Viewgraph #17:

This is a photograph of the scuff plates showing the lack of atomic oxygen shadows from the trunnions.

C-2

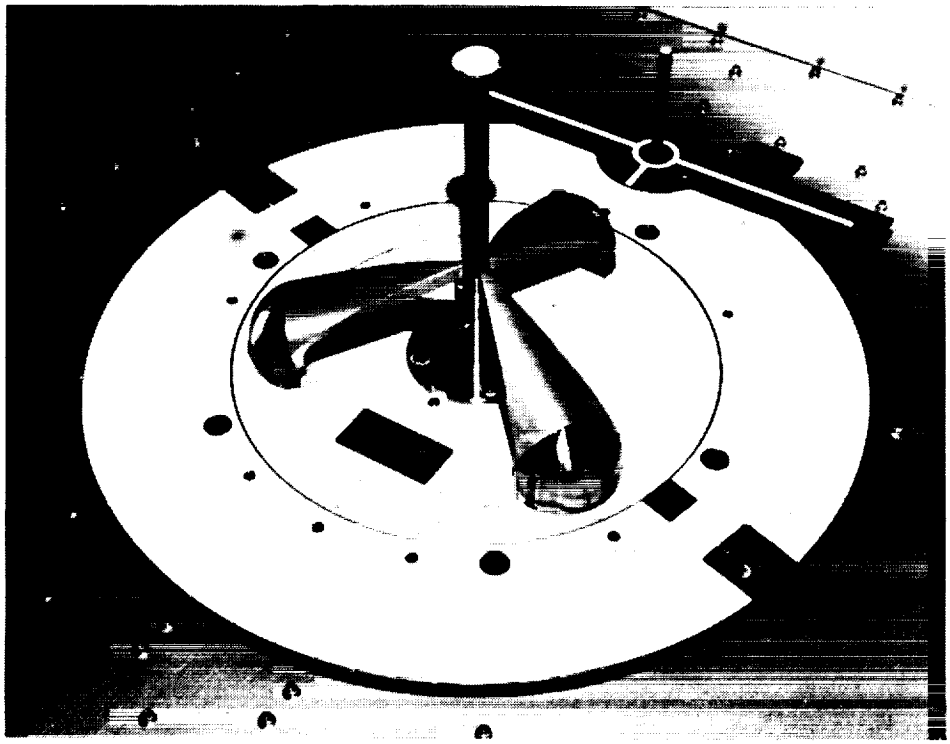

Viewgraph #18:

This is a photo of the grapple fixture which did not reveal atomic oxygen shadows from the grapple alignment pin.

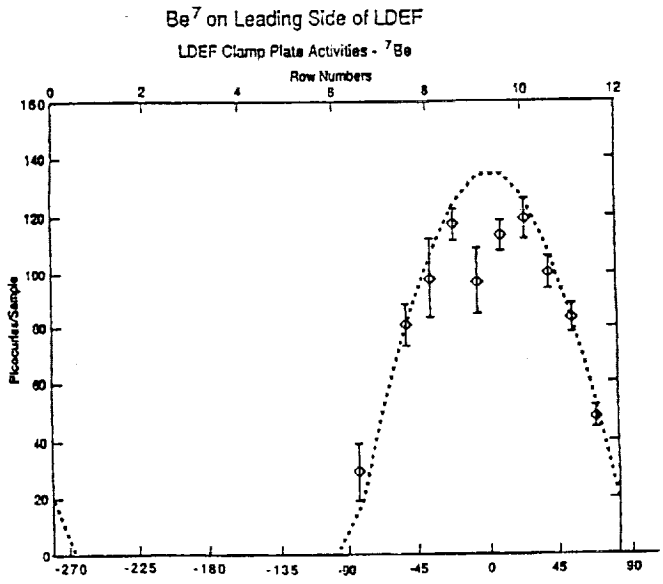

Viewgraph #19:

The Be^7 calculation as a function of angle around LDEF held potential to determine pitch angle information if space or earth end data was taken. However, because no such data was taken, correlations with this plot were not possible.

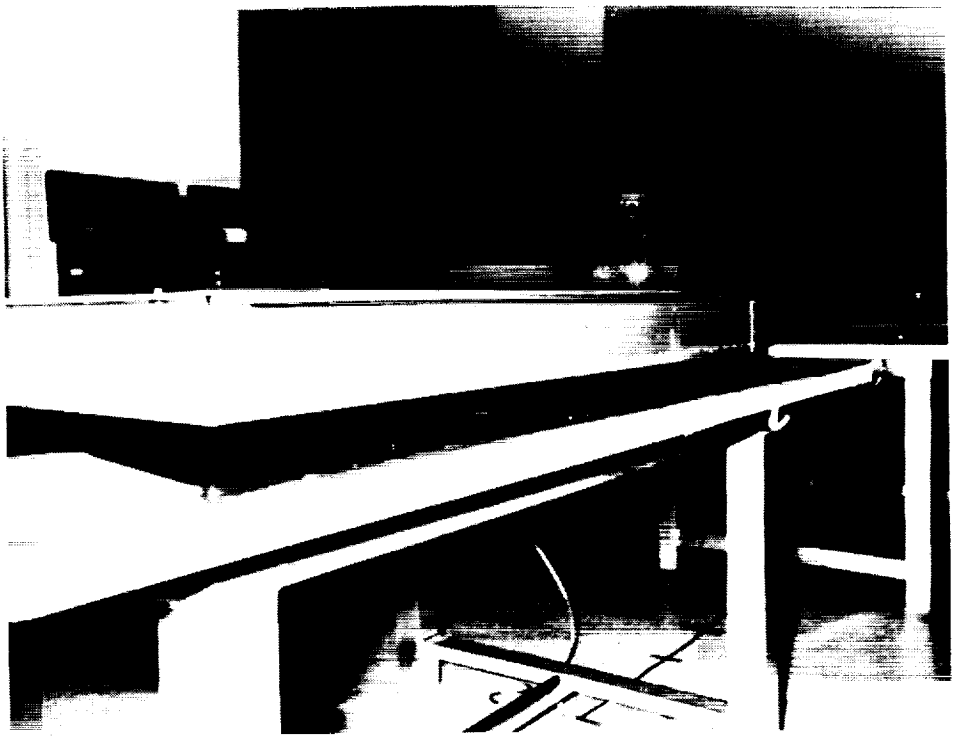

Viewgraph #20:

This is a photograph of the tray 9C showing atomic oxygen streaks on the sides of the tray as a result of its entrance through 10-32 screw holes from the nut plates on the tray flanges. The streaks were found to contain silicon, which is thought to be in the form of silicates as a result of atomic oxygen interaction with arriving silicone contaminants.

ORIGINAL PAGE
BLACK AND WHITE PHOTOGRAPH

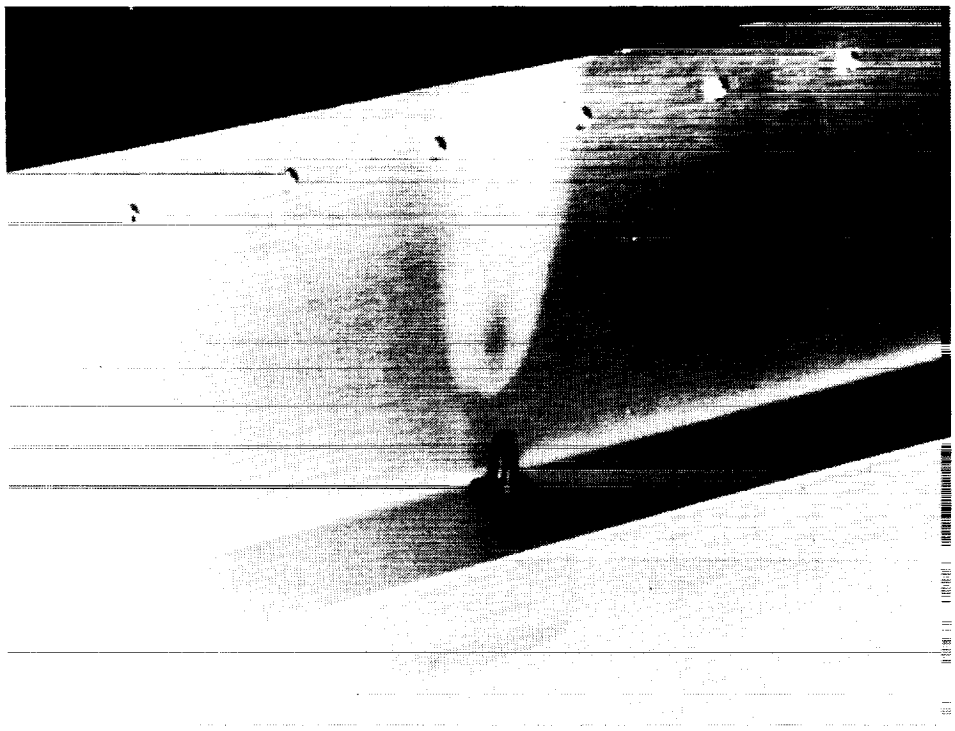

Viewgraph 21:

This is a photograph of the row 10 side of tray 9C showing the ground atomic oxygen streak associated with the nut plate aperture. Such streaks were used to calculate the pitch angle for LDEF.

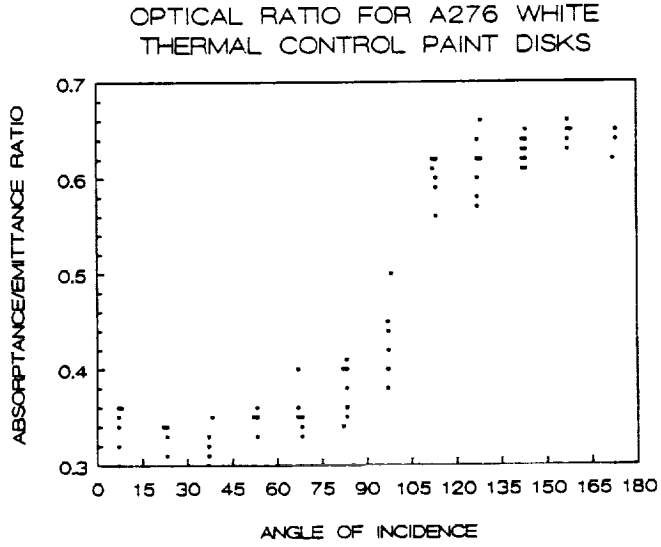

Viewgraph #22:

This plot shows the solar absorptance-to-thermal emittance ratio as a function of position around LDEF for A276 white thermal control paint disks. Through knowledge of the earth and space end thermal control paint solar absorptance-to-thermal emittance ratio, one can estimate the angle of the surface with respect to the ram direction.

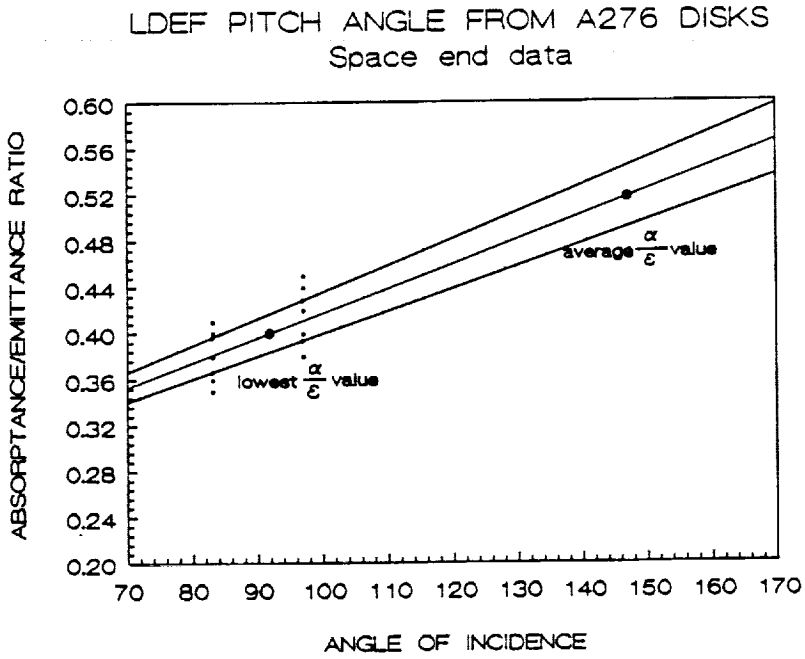

Viewgraph #23:

The small dots near 90° angle of incidence are the solar absorptance-to-thermal emittance ratio of the paint spots closest to 90° angle of incidence, or a zero pitch offset. As can be seen from the photo, paint spots from the space end with the lowest alpha over epsilon value or average alpha over epsilon value, produced a greater than 90° angle of incidence, which implies pitch angles of -1.72 or -56.9°. The wide variation between the lowest and the average alpha over epsilon value is probably a result of the widely varying level of contamination on the space end, which also currently contributes to the lack of reliability of this measurement.

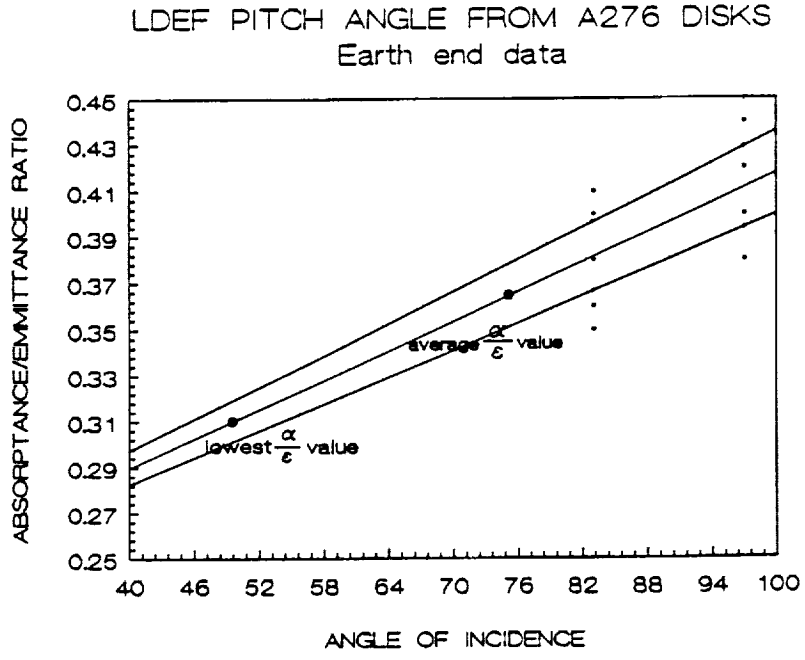

Viewgraph #24:

The earth end and data produced pitch angles which were also highly negative and with large uncertainties. The highly negative pitch angles are probably a result of the earth end surfaces being cleaner, possibly as a consequence of lower contamination, or being warmer. Thus the earth end paint spot data cannot be highly relied upon.

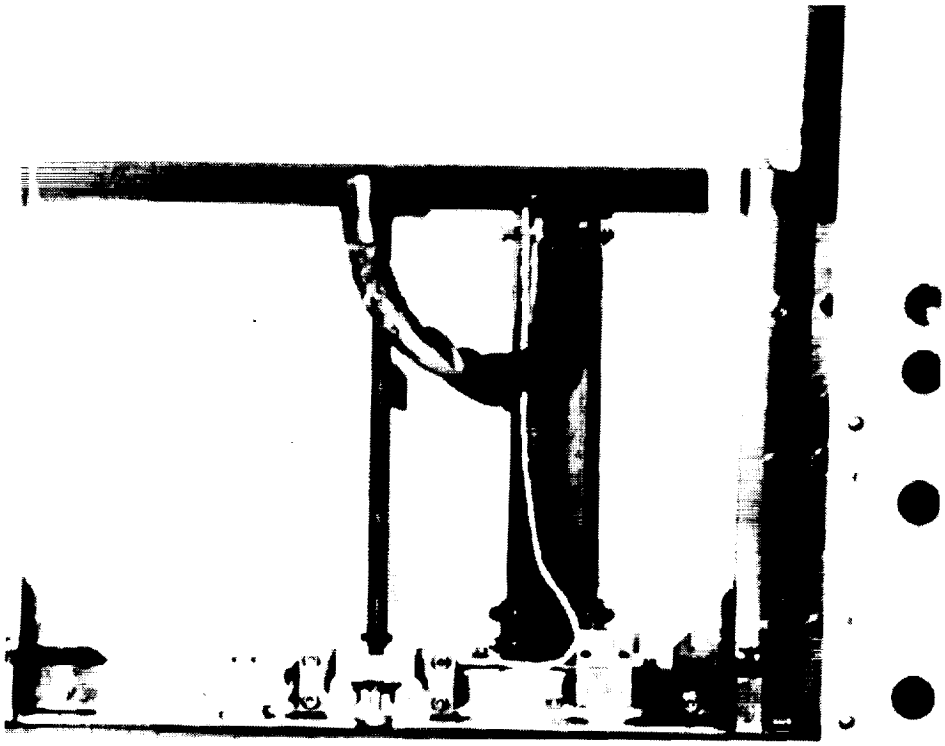

Viewgraph #25:

The experiment exposure control canister drive screw did not produce atomic oxygen shadows. Shadows shown in this figure are a result of room illumination, rather than atomic oxygen interactions.

LDEF PITCH ANGLE

Generic Measurement	
Pinhole Camera from AO114 on 9C	1.0 ± 0.4
Nut Plate Shadows on Tray Sides Parallel to Longerons on Tray 9C	0.66 ± 0.35
Average	0.8 ± 0.4

Viewgraph #26:

This table summarizes the LDEF pitch angle data which is considered meaningful for calculation of an overall average pitch angle of 0.8 ± 0.4°, where the overall average pitch angle is a weighted average of the two generic types of measurements which provided meaningful data, and the uncertainty is the probable error.

SUMMARY

	Degrees	
LDEF YAW OFFSET	8.1 ± 0.6	(Allowing higher atomic oxygen exposure of Row 12 than planned)
LDEF PITCH OFFSET	0.8 ± 0.4	(space end tipped forward)

Viewgraph #27:

This table summarizes the final LDEF yaw and pitch offset angles and their associated probable errors.

Effect of Yaw and Pitch Offset on Atomic Oxygen Fluence

Location	Fluence Relative to Zero Offset
Row 12	2.16
Row 6	0.13
Space End	1.18
Earth End	0.87

Viewgraph #28:

This table illustrates the consequences of the yaw and pitch offset on surfaces which are most affected by the LDEF misorientation. As can be seen, the yaw offset effects have far greater relative changes on the atomic oxygen fluence than the smaller pitch offset does.

LDEF Contamination

Co-Chairmen: Wayne Stuckey and Steve Koontz
Recorder: Russell Crutcher